

# From Filters to VLMs: Benchmarking Defogging Methods through Object Detection and Segmentation Performance

Ardalan Aryashad, Parsa Razmara<sup>\*</sup>, Amin Mahjoub,  
Seyedarmin Azizi, Mahdi Salmani, Arad Firouzkouhi  
University of Southern California

## Abstract

Autonomous driving perception systems are particularly vulnerable in foggy conditions, where light scattering reduces contrast and obscures fine details critical for safe operation. While numerous defogging methods exist—from handcrafted filters to learned restoration models—improvements in image fidelity do not consistently translate into better downstream detection and segmentation. Moreover, prior evaluations often rely on synthetic data, leaving questions about real-world transferability. We present a structured empirical study that benchmarks a comprehensive set of pipelines, including (i) classical filters, (ii) modern defogging networks, (iii) chained variants (*filter*→*model*, *model*→*filter*), and (iv) prompt-driven visual–language image editing models (VLM) applied directly to foggy images. Using Foggy Cityscapes, we assess both image quality and downstream performance on object detection (mAP) and segmentation (PQ, RQ, SQ). Our analysis reveals when defogging helps, when chaining yields synergy or degradation, and how VLM-based editors compare to dedicated approaches. In addition, we evaluate qualitative rubric-based scores from a VLM judge and quantify their alignment with task metrics, showing strong correlations with mAP. Together, these results establish a transparent, task-oriented benchmark for defogging methods and highlight the conditions under which preprocessing genuinely improves autonomous perception in adverse weather.

## 1. Introduction

Autonomous driving perception degrades markedly in fog, where scattering reduces contrast and masks fine structure, impairing detection and segmentation of safety–critical objects (e.g., pedestrians, vehicles, signage) [4, 40, 41]. Many defogging approaches exist, ranging from classical filters [13, 36] to modern learned restorers[5, 25, 35]; how-

ever, improvements in image appearance do not consistently translate into better downstream perception [25, 40]. Moreover, much prior evaluation emphasizes synthetic benchmarks, leaving open questions about transfer to realistic driving scenes [27].

This paper presents a structured empirical study that compares a comprehensive set of processing pipelines under a consistent evaluation stack: (i) raw foggy input, (ii) handcrafted filters, (iii) learned defogging models, (iv) chained pipelines (*filter*→*model* and *model*→*filter*), and (v) visual–language–model (VLM) image editing. We quantify not only image appearance but also *downstream* object detection and segmentation performance[6, 21] on Foggy Cityscapes[40], enabling an end-to-end view of whether, when, and how defogging helps what autonomous vehicle (AV) systems actually need. Figure 1 shows an example of detecting an object that was masked by the fog.

We target two persistent gaps: (i) over–reliance on pixel-level fidelity scores as proxies for downstream task performance [27], and (ii) limited evidence on how generic, prompt-driven VLM editors [8, 24, 45] compare to dedicated defogging models or simple filters when judged by detection/segmentation accuracy. Our design isolates these factors by holding the detection/segmentation module fixed and varying only the preprocessing pipeline, including mixed chains that test for complementarity. In addition, we conduct a *qualitative assessment using a VLM judge* applied to model outputs and analyze its *alignment with quantitative metrics*, measuring whether rubric-based VLM scores correlate with downstream detection (mAP) [21].

We introduce a tailored chain-of-thought (CoT) defogging prompt for general-purpose image-editing back-ends in image-to-image mode. The prompt explicitly qualitative cues such as edge acuity, local contrast, color fidelity, artifact suppression, and semantic consistency, together with a negative prompt that suppresses common failure modes (e.g., leftover fog, glow/halo, blur, exposure errors, hallucinations). Across Foggy Cityscapes, the CoT prompt yields consistent mean average precision (mAP) gains over a minimal baseline prompt and improves segmentation quality,

<sup>\*</sup>Corresponding author: prazmara@usc.edu



Figure 1. Example showing how defogging improves downstream object detection by restoring visibility of fog-obscured objects.

while classical filters and simple chains offer mixed benefits. Qualitative rubric scores for edge sharpness and local contrast show the strongest correlation with mAP, indicating that aligning prompts with task-salient visual cues translates into downstream detection improvements.

We summarize our *contributions* as follows:

- we do a large-scale, apples-to-apples comparison of handcrafted filters, learned defogging models, chained variants, and VLM editing for foggy driving scenes, evaluated on *downstream* detection and segmentation.
- We analyze mixed pipelines (*filter*→*model*, *model*→*filter*) that reveals when chaining helps or hurts relative to single-stage methods.
- As part of the pipeline, we conduct a prompt-engineering evaluation for VLM editors aligned to detector-salient cues, contrasting minimal vs. chain-of-thought prompts and negatives.
- An experimental study of **VLM-metric alignment** is done to quantify how well qualitative VLM scores track task metrics (mAP) via correlation analyses, highlighting when cosmetic improvements do or (do not) translate to task gains.
- We provide a transparent evaluation protocol (datasets, splits, detector/segmenter, and metrics) to support reproducibility and future comparisons (details in Sections 3, 4).

Section 2 reviews prior work on classical filters, learned defogging, datasets, and task-driven approaches. Section 3 details our pipelines, metrics, and qualitative VLM assessment rubric; Section 4 covers datasets and evaluation frameworks; Sections 5, 6 report results and ablations, followed by conclusions in Section 7. Code and benchmark resources are publicly available at <https://github.com/prazmara/defog-detection-benchmark>.

## 2. Related Work

**Classical priors and image processing.** Early single-image dehazing was dominated by priors and enhancement filters. The Dark Channel Prior (DCP) [13] remains the most influential, but suffers from haloing, color shifts, and failures in sky regions [33]. Other handcrafted approaches,

such as Multi-Scale Retinex [36, 37] and CLAHE [49], improve visibility by boosting local contrast or dynamic range but often amplify noise and distort colors [16]. While fast and lightweight, these methods lack physical grounding and can harm downstream recognition.

**Learning-based dehazing.** CNNs shifted the field from physics-based priors to data-driven restoration. DehazeNet [5] learned transmission maps, while AOD-Net [25] enabled joint optimization with detectors. Later works such as GridDehazeNet [28] and FFA-Net [35] improved spatial adaptivity. However, CNN models trained on synthetic data often generalize poorly to real fog and may introduce perceptual artifacts misaligned with task features.

**Transformer-based models.** Recent vision transformers capture long-range dependencies and deliver state-of-the-art dehazing quality. DehazeFormer [42] and follow-ups on frequency modeling and UHD restoration [47, 48] improve perceptual fidelity on synthetic benchmarks. Yet, they still struggle in dense or real-world haze and risk hallucinating textures, raising concerns for safety-critical perception.

**Datasets and benchmarks.** RESIDE [27] established large-scale evaluation protocols, while Foggy Cityscapes [40] and ACDC [41] focus on driving scenarios. Seeing Through Fog [4] extends this to multimodal sensing. Despite their impact, synthetic datasets dominate, and models trained on them often fail to generalize to real fog.

**Impact on downstream tasks.** The benefit of dehazing for detection/segmentation is mixed. AOD-Net showed gains when trained jointly with Faster R-CNN [25], but Sakaridis *et al.* found preprocessing alone can degrade segmentation due to artifacts [40]. Fusion studies [4] suggest that dehazing is insufficient in severe conditions. Selective enhancement may help foggy scenes but harm clear ones, motivating condition-aware application.

**Task-driven and generative approaches.** Task-aware models optimize directly for recognition, including united dehazing-detection pipelines [26], detection-friendly dehazing [9], and domain adaptation for foggy segmentation [18, 30]. While effective, they remain dependent on synthetic supervision and domain heuristics. More re-

cently, diffusion and vision–language models offer flexible prompt-driven “defogging,” but lack physical grounding and often hallucinate content, making them more suitable for augmentation than robust perception. In addition to architectural and training choices, decoding strategies influence reliability: unconstrained sampling can lead to neural text degeneration [15], while bounded-entropy schemes such as Top-H Decoding offer a controllable balance between coherence and creativity [34].

**Broader cross-domain advances** The challenges we identify in defogging, such as balancing efficiency, robustness, and task-driven utility, echo broader trends across machine learning. For example, efficient learning methods have long been central, from model compression [12] to green approaches for low-level vision [32]. Architectural innovations such as graph neural networks [20] and DAG-based convolutions [39] demonstrate how structure-aware design can improve generalization and robustness in perception tasks. Similar principles are seen in domain-specific applications, where vision-language and generative models are applied in finance [19] and medical imaging [11, 38], and predictive modeling supports advances in healthcare [1, 2]. Finally, fairness-aware methods [10, 31] highlight the need for trustworthy deployment. These parallel efforts emphasize that progress across domains depends not only on fidelity or accuracy, but also on delivering reliable, efficient, and fair outcomes, which motivates our benchmarking of defogging pipelines.

**Summary.** Classical priors are fast but brittle, CNN-transformer restorers excel on benchmarks but face real-world gaps, and generic preprocessing is not always task beneficial. Task-driven pipelines and larger real-world datasets appear essential for reliable deployment.

### 3. Methodology

Motivated by the need to measure *downstream task performance* on the dehazed images rather than only pixel fidelity, our methodology fixes the detection/segmentation module and varies only the defogging pipelines. We compare classical filters, modern learned restorers, chained variants (*filter* → *model* and *model* → *filter*), and training-free and training-based VLM image editing steered by a tailored CoT prompt. Experiments are run on Foggy Cityscapes, and we report object detection (mAP) and segmentation (PQ/RQ/SQ) alongside a qualitative rubric that targets detector-salient cues.

This section details three components. Section 3.1 (*Quantitative Evaluation Pipeline*) specifies datasets, pipelines, and metrics, holding the evaluator fixed while swapping defogging pipelines. Section 3.2 (*Qualitative Evaluation Pipeline*) introduces a VLM judge with a rubric over edge acuity, local contrast, color fidelity, artifact suppression, and semantic/relational consistency, and analyzes

its alignment with quantitative metrics. Section 3.3 (*Prompt Engineering and Model Evaluation*) formalizes our prompt design. Each editor runs in image-to-image mode without training, and for every image we generate two edits that differ only in the prompt: a minimal baseline and a CoT prompt paired with a negative prompt. The CoT prompt decomposes the operation (remove fog → sharpen boundaries → boost local contrast → photometric check), explicitly names safety-critical categories (cars, pedestrians, traffic signs, buildings), and enforces natural lighting and realistic colors. The negative prompt enumerates failure modes (leftover fog, glow/halo, blur, exposure errors, hallucinations) to suppress artifacts. Inference controls (resolution, guidance, steps, seed) are fixed to isolate prompt effects.

#### 3.1. Quantitative Evaluation Pipeline

**Defogging pipeline** we used the validation split of the Foggy Cityscapes dataset. Specifically, for the experiments reported here we select the medium intensity fog images as input to the pipelines, so as to assess the performance in a nontrivial but not extreme visibility degradation setting. First, we apply each of the handcrafted filters individually (DCP, CLAHE, MSR). These filtered images are stored to be used later in our pipeline. Second, we subject the foggy images to dedicated defogging models (DehazeFormer, MITNet, focalnet) to produce model restored images. In addition we examine mixed pipelines in two configurations:

- Filter → Model: applying a handcrafted filter first, then feeding the filtered image into one of the defogging models
- Model → Filter: applying the model first, then refining via a handcrafted filter

In addition, we also process the original foggy images using VLM-based editing systems (such as Nano Banana [43], Flux [3]) via prompt engineering. This full set of pipelines allows us to compare not just image appearance metrics, but downstream perception performance under consistent inputs.

**Object Detection Metric** To evaluate the effectiveness of the defogging methods with respect to object detection, we used the mAP metric. Mean Average Precision is a standard metric in the object detection literature measuring how accurately a model locates and classifies objects across all classes. It is defined by computing the Average Precision (AP) for each object class over a range of confidence thresholds, and then averaging those class-wise APs to yield mAP. In our study, we use the YOLOv111 model as the detector across all pipelines: for each processed image, we run YOLOv111 to obtain detection bounding boxes with class predictions and confidence scores. We then compute mAP for annotated object categories present in the Cityscapes Foggy validation set, matching model predic-

tions to ground-truth annotations. By comparing the mAP of the YOLOv111 on the raw foggy images to that on each defogged output, we quantify both the degradation caused by fog and the performance gains - if any - afforded by each defogging method or pipeline.

**Segmentation Metric** In addition to object detection, we also evaluate segmentation, with a focus on panoptic segmentation [21]. Panoptic segmentation labels every pixel with a semantic class and assigns an instance ID to each countable object; amorphous (“stuff”) regions receive only a class label. For comparison, semantic segmentation [17, 29, 46] assigns class labels to pixels but does not distinguish different objects of the same class, while instance segmentation [14] predicts a separate mask (and class) for each individual object. To compare segmentation outputs, we report *Panoptic Quality* (PQ) and its components *Segmentation Quality* (SQ) and *Recognition Quality* (RQ). Let  $TP$ ,  $FP$ , and  $FN$  denote the counts of true positives, false positives, and false negatives under one-to-one IoU matching with threshold  $\tau$  (we use  $\tau=0.5$ ). A true positive is a matched prediction–ground-truth pair with  $\text{IoU} \geq \tau$ ; a false positive is an unmatched prediction; a false negative is an unmatched ground-truth segment. Then

$$\text{RQ} = \frac{TP}{TP + \frac{1}{2}FP + \frac{1}{2}FN} \quad (1)$$

$$\text{SQ} = \frac{1}{TP} \sum_{(p,g) \in \mathcal{M}} \text{IoU}(p,g), \quad (2)$$

$$\text{PQ} = \text{SQ} \times \text{RQ} \quad (3)$$

where  $\mathcal{M}$  is the set of matched pairs. Intuitively, SQ measures overlap quality of matched masks, RQ measures detection and association, and PQ increases with better overlaps and fewer errors.

### 3.2. Qualitative Evaluation Pipeline

**Rationale for reporting qualitative metrics.** Cityscapes images have a resolution of  $2048 \times 1024$  pixels, whereas many image-editing models operate only on smaller or square inputs and cannot directly generate  $2048 \times 1024$  outputs. Quantitative scores such as mAP are designed to measure how well detector predictions match ground-truth bounding boxes. However, when an image is resized, even with aspect ratio preserved, the exact pixel locations of objects shift slightly relative to the ground truth. Since detectors like YOLO evaluate predictions against fixed bounding boxes stored in absolute pixel coordinates, these shifts cause mismatches that lead to incorrect mAP values, even if object visibility has actually improved. Two practical workarounds are possible. One is to split the input into left and right halves of  $1024 \times 1024$ , process each half separately, and then stitch them back together. This approach

preserves resolution and alignment with the ground truth, but after defogging, the two halves often differ in brightness or color, leaving a visible boundary at the seam.

The other option is to preserve the 2:1 aspect ratio, generate a smaller image, resize (up-sample) it back to  $2048 \times 1024$ , and then rely on *qualitative evaluations* that assess how clear and realistic the defogged image appears without requiring exact pixel-level alignment. To avoid splitting artifacts and overcome the sensitivity of YOLO-style pipelines to small coordinate shifts, we adopt qualitative scoring as a complementary measure to the standard mAP score. This captures the intended effects of defogging—such as sharper edges, stronger contrast, and more realistic colors—when detector scores are not reliable by resolution limitations.

**Qualitative Scoring with VLMs** A Vision-Language Model is employed as a judge to assess the perceptual quality of defogged outputs. Each evaluation is structured as a triplet consisting of the candidate defogged image, the corresponding ground-truth clear image, and the original foggy input.

**Rubric Generation** The evaluation rubric was adapted from prior VLM-based assessment studies [23]. The VLM is prompted with six axes:

1. **Visibility Restoration of Objects:** recovery of objects and background details across near, mid-range, and far depths.
2. **Boundary Clarity:** sharpness and definition of object contours.
3. **Scene Consistency:** preservation of global geometry, layout, and spatial relationships.
4. **Object Consistency:** agreement with ground truth in counts and categories of major objects such as cars, pedestrians, and traffic lights.
5. **Perceived Detectability:** judgment of how easily a detector could find objects compared to the foggy input.
6. **Relation Consistency:** similarity of object relations, including positions, alignments, and interactions, between ground truth and candidate.

For each axis, the VLM outputs a score on a 1–5 scale. To ensure consistent and reproducible judgments across all models, prompts explicitly constrained the VLM to follow this rubric for every image.

### 3.3. Prompt Engineering and Model Evaluation

We investigate whether lightweight prompt engineering can steer general-purpose visual language/image editing models toward defogged outputs that improve downstream task. Our design aligns prompt content with detector-salient cues (edge acuity, local contrast, color fidelity, artifact suppression, semantic consistency) and measures impact on mAP using a fixed evaluation stack (Sec. 4).

We run the image editing models in image-to-image

mode, without any extra training. For each input frame, we generate two edited variants that differ *only* in the prompt: a minimal baseline prompt and a CoT prompt paired with a negative prompt.

**Rubric-guided CoT design.** Before finalizing the CoT text, we scored a subset of images with a VLM judge and computed Pearson correlations between rubric axes and mAP. The strongest associations were *boundary clarity*, *visibility restoration*, and *perceived detectability*. We therefore emphasized sharp boundaries, higher local contrast, and clear presentation of traffic-critical objects in the CoT wording. See Section 6 for details of the correlation analysis.

**Design rationale (CoT):** The CoT prompt decomposes the edit into an explicit micro-plan (*remove fog* → *sharpen boundaries* → *boost local contrast* → *check photometric realism*), names safety-critical categories (cars, pedestrians, traffic signs, buildings) to focus enhancement where detectors are most sensitive, and anchors photometry with “natural lighting” and “realistic colors” to reduce colorimetric drift. The negative prompt enumerates common failure modes (leftover fog, glow/halo, blur, exposure errors, stylization, hallucinations, artifacts/noise) that degrade detection features.

**Reproducibility.** We expose the exact strings to ensure reproducibility and to standardize comparisons across editors. In addition, we fixed the sampling method, guidance scale, and number of inference steps for each editor. We also fix the random seed to ensure reproducibility across runs.

#### CoT Prompt (VLM Defogging for Detection)

Remove fog step by step, mist, and atmospheric haze. Produce a crystal-clear image with sharp object boundaries and high local contrast. Ensure cars, pedestrians, traffic signs, and buildings are distinctly visible with accurate shapes, edges, and textures. Preserve natural lighting and realistic colors. Photo-realistic; optimized for object detection.

#### Negative Prompt (Failure Modes to Suppress)

*Short description:* Suppresses leftover fog and generative artifacts that harm detector features (blur, glow, color drift, hallucinations, compression artifacts).

fog, haze, mist, blur, soft edges, low contrast, washed out colors, glow, bloom, overexposure, underexposure, unrealistic textures, oversaturation, artistic stylization, distortion, hallucinated objects, artifacts, noise

#### Baseline Prompt (No CoT)

Need to remove fog

## 4. Experiments

### 4.1. Dataset Preparation

For the experiments, we utilize the Foggy Cityscapes dataset, selecting only the medium fog density images corresponding to  $\beta = 0.01$  among the fog intensities defined in the dataset. The Cityscapes dataset includes fine annotation versions for all splits: training, validation, and test as well as “clear” (ground truth) images and foggy versions at varying  $\beta$  values. To make the dataset suitable for object detection benchmarking, we extract the fine annotation masks and polygonal segmentation labels and convert them into the COCO “instances” format (JSON) containing bounding boxes. Following prior conversion tools (e.g., the Cityscapes-to-COCO conversion scripts by Till-Beemelmanns) that filter for relevant object classes such as ‘person’, ‘car’, ‘truck’, ‘bus’, ‘train’, ‘motorcycle’, and ‘bicycle’, we similarly limit the COCO JSON annotations to these classes. Polygon and mask data from the fine annotation files are processed: instances are converted to bounding boxes with image metadata, image dimensions, and image to annotation mappings created consistent with COCO.

### 4.2. Defogging Pipelines

We constructed multiple defogging pipelines combining handcrafted filters, dedicated defogging models, and VLMs to explore their efficacy both in isolation and in chain combinations. Overall, the mentioned combinations in methodology section yield a total of 54 distinct datasets: comprising filter-only results, model-only outputs, filter-then-model chains, model-then-filter chains, and VLM output variations over prompt settings. Moreover, we perform additional experiments in which we train the DehazeFormer model directly on Cityscapes (foggy and clear pair) images, to assess the performance on synthetic datasets and then demonstrate its effectiveness on real world images.

As a training-based baseline VLM, we adopt `stable-diffusion-xl-base-1.0` as the diffusion backbone for defogging, combined with ControlNet to condition the diffusion process on foggy images. For training, we follow the setup provided in the HuggingFace ControlNet training pipeline [8], using the Foggy Cityscapes training split as the dataset. The corresponding clean images are used as inputs to the diffusion model, and the end-to-end pipeline is trained with the baseline prompt defined in 3.3 as the text input stream. The model is trained for 10 epochs on the entire training split.

### 4.3. Detection Evaluation Framework

To perform detection evaluation across all the processed datasets, we employ the FiftyOne Python library [44], which offers facilities for loading externally annotated datasets in COCO format, applying object detection models (such as YOLO variants), visualizing predictions, and computing evaluation metrics per class and overall. For each of the 54 processed image sets, the corresponding COCO JSON annotation file is loaded via FiftyOne, together with the images. We then run the YOLOv111 detector on every image in each dataset, saving the predicted bounding boxes, confidence scores, and predicted categories. FiftyOne is used to overlay predictions on images, and also to aggregate prediction vs. ground truth matches and compute overall detection metrics (e.g. mAP). FiftyOne’s capacity to visualize results enables rapid iteration: we can quickly compare detection outputs for filtered vs. model outputs vs. VLM outputs, aiding in prompt engineering and pipeline selection.

### 4.4. Segmentation Evaluation Framework

For segmentation, we use Mask2Former [6] pretrained on Cityscapes [7]. The model combines a multi-scale pixel decoder with a transformer decoder that predicts a fixed set of mask queries; each query yields a class label and an associated mask via masked attention. The resulting scored masks are composed into the segmentation output. For reproducibility, we rely on the public Mask2Former implementation and checkpoints hosted on the Hugging Face Hub [24, 45]. After generating predictions on each dataset, we evaluate the segmentation using the COCO toolkit [22].

### 4.5. Qualitative Data Gathering

To obtain human-like judgments of our defogged results, we employed GPT-4o-mini in an LLM-as-a-judge evaluation framework. To ensure reproducibility, the temperature was fixed at zero. In addition, we designed a strict evaluation rubric that the model was required to follow when assigning scores to each image. For each candidate model, GPT-based qualitative scores were collected on approximately 300 sampled images. Scores across the rubric axes were averaged to produce a stable summary for each model. The aggregated results aligned with both mAP and judge ratings of defogged outputs.

## 5. Results

In Table 1, we present the performance of various defogging pipelines on object detection and segmentation, along with the change relative to baseline foggy images. The “Change (mAP)” column quantifies how much each pipeline improves or degrades the mean Average Precision compared to the foggy baseline at  $\beta = 0.01$ . In other words, the

change is computed by dividing the difference of mAP of each pipeline with the mAP of foggy image ( $\beta = 0.01$ ) to the difference of mAP between foggy image and ground truth. A positive change indicates that the pipeline yields better detection performance. Or in other words the defogging (single operations, or the chain of operations) is helpful whereas a negative change indicates performance worse than baseline. For example, the DehazeFormer-trained pipeline with no additional filter yields +98.87% change in mAP, very close to “ground-truth,” whereas some pipelines using weaker models or filters show only modest gains or even negative changes.

$$\text{Change} = \frac{mAP_{\text{Pipeline}} - mAP_{\text{Foggy}}}{mAP_{\text{GT}} - mAP_{\text{Foggy}}} \times 100 \quad (4)$$

Reading across the “Base” and “Next Step” columns shows whether an operation is the base method or applied after that. When another method appears under “Next Step”, it indicates that after performing the base, that filter or model is applied; “None” means only the base method is used. The data reveal that applying a strong defogging model (DehazeFormer trained on Foggy Cityscape) tends to produce the largest gains. Further, combining models and filters shows that model  $\rightarrow$  filter often yields better improvement than filter  $\rightarrow$  model, contrary to what one might expect. For example, the pipeline “DehazeFormer  $\rightarrow$  CLAHE” yields +56.60% improvement, outperforming the “CLAHE  $\rightarrow$  DehazeFormer” with 43.40% change. A plausible hypothesis for this trend is that allowing the model to handle the fog first, followed by applying a filter, helps refine image edges and correct color inconsistencies. Consequently, pipelines in which the model acts first and the filter is applied afterward tend to maximize detection and segmentation performance under foggy conditions.

## 6. Ablation and Discussions

**Qualitative evaluation.** As shown in Table 2, the qualitative rubric confirms these trends. Among editing-based approaches, *Flux CoT (Resized)* consistently scores higher than *Flux CoT (Split)* across visibility restoration, perceived detectability, and the overall total, indicating that resizing back to  $2048 \times 1024$  is preferable to left/right tiling for perceptual quality. The split variant also exhibits larger variance, consistent with seam and exposure inconsistencies. The trained DehazeFormer achieves the best boundary clarity and the highest or near-highest total, closely followed by *Flux CoT (Resized)*, whereas non-CoT prompts and split outputs lag behind. Overall, the table shows three clear patterns: (i) CoT non-CoT within the same editor, (ii) Resized Split for the same prompt, and (iii) the trained DehazeFormer remains a strong baseline, but CoT-guided editing (Resized) approaches its qualitative scores and clearly outperforms Split and non-CoT variants, indicating that step-

Base	Next Step	mAP $\uparrow$	PQ $\uparrow$	RQ $\uparrow$	SQ $\uparrow$	Change (mAP)
Ground-Truth (GT)	None	<b>0.2560</b>	<b>100.0</b>	<b>100.0</b>	<b>100.0</b>	Reference
Fog Density $\beta = 0.01$	None	0.2295	57.9	69.3	83.1	Reference
DehazeFormer Trained	None	<b>0.2557</b>	<b>74.4</b>	<b>83.9</b>	<b>88.4</b>	+98.87%
	CLAHE	0.2555	70.3	81.3	86.3	+98.11%
	MSR	0.2530	59.4	81.9	71.9	+88.68%
	DCP	0.2452	69.9	81.2	85.9	+59.25%
DehazeFormer	None	0.2379	63.0	74.2	<b>84.6</b>	+31.70%
	CLAHE	<b>0.2445</b>	62.4	74.4	83.4	+56.60%
	DCP	0.2409	<b>64.2</b>	<b>76.1</b>	83.8	+43.02%
	MSR	0.2336	59.4	71.9	81.9	+15.47%
CLAHE	None	0.2383	58.0	<b>82.4</b>	69.9	+33.21%
	DehazeFormer Trained	<b>0.2505</b>	<b>69.9</b>	81.1	<b>85.9</b>	+79.25%
	DehazeFormer	0.2410	61.1	73.1	83.2	+43.40%
	FocalNet	0.2385	60.9	73.1	82.8	+33.96%
	MITNet	0.2328	56.1	67.9	82.1	+12.45%
MSR	None	0.2318	50.7	<b>79.8</b>	62.9	+8.68%
	DehazeFormer Trained	<b>0.2435</b>	<b>53.2</b>	65.6	80.5	+52.83%
	DehazeFormer	0.2343	51.5	63.9	79.8	+18.11%
	FocalNet	0.2351	51.7	64.2	79.9	+21.13%
	MITNet	0.2338	57.9	69.3	<b>83.1</b>	+16.23%
DCP	None	0.2369	64.0	<b>83.4</b>	76.3	+27.92%
	DehazeFormer Trained	<b>0.2376</b>	<b>64.8</b>	77.0	<b>83.8</b>	+30.57%
	DehazeFormer	0.2345	64.2	76.1	<b>83.8</b>	+18.87%
	MITNet	0.2358	59.5	71.5	82.4	+23.77%
	FocalNet	0.2347	63.6	75.9	83.2	+19.62%
FocalNet	None	0.2353	62.6	74.2	<b>84.0</b>	+21.89%
	CLAHE	<b>0.2385</b>	60.4	72.3	83.1	+33.96%
	DCP	0.2356	<b>62.8</b>	<b>74.7</b>	83.5	+23.02%
	MSR	0.2171	51.7	64.2	79.9	-46.79%
MITNet	None	0.2251	<b>57.9</b>	<b>69.3</b>	<b>83.1</b>	-16.60%
	CLAHE	<b>0.2279</b>	56.1	67.9	82.1	-6.04%
	DCP	0.2238	56.8	68.4	82.6	-21.51%
	MSR	0.2151	51.0	63.3	79.7	-54.34%
Flux	COT	<b>0.2376</b>	<b>59.7</b>	82.8	<b>71.7</b>	+30.57%
	Not COT	0.2306	55.5	<b>83.4</b>	66.4	+4.15%
ControlNet	None	<b>0.2009</b>	<b>79.2</b>	75.6	63.6	-107.92%
NanoBanana	None	0.1941	61.2	<b>83.0</b>	<b>73.5</b>	-133.58%

Table 1. Performance of Various Defogging Pipelines on Object Detection and Segmentation Metrics

wise, detection-aware prompting delivers perceptual improvements that matter when detector metrics are unreliable at non-native resolutions. Using the totals in Table 2 and the mAP values in Table 1, we compute the Pearson correlation between qualitative score and mAP across models. The correlation is strong ( $r = 0.94$ ; Figure. 3), indicating that the qualitative rubric tracks the same task-

relevant improvements that boost detection accuracy. Thus, it serves as a reliable, complementary indicator of object-detection utility, especially when detector-based evaluation is confounded by resolution constraints. Across individual rubric axes, *boundary clarity* ( $r \approx 0.84$ ), *perceived detectability* ( $r \approx 0.83$ ), and *visibility restoration* ( $r \approx 0.83$ ) exhibit the highest correlation with mAP, while scene/object-

Method	visibility restoration	boundary clarity	scene consistency	object consistency	perceived detectability	relation consistency	Total
Ground Truth (GT)	4.95	4.95	5.00	5.00	4.95	5.00	29.85
Dehazeformer Trained	4.07	<b>3.96</b>	4.59	4.86	4.07	4.81	26.36
Flux COT (Resized)	<b>4.51</b>	3.95	4.06	4.74	<b>4.38</b>	4.58	26.21
Flux COT (Split)	4.08	3.89	3.64	4.01	4.06	4.02	23.70
NanoBanana	2.44	2.44	4.37	4.50	2.44	4.52	20.71
Dehazeformer	2.17	2.17	4.54	4.67	2.18	4.67	19.82
Flux Not COT (Resized)	1.60	1.58	<b>4.81</b>	<b>4.90</b>	1.60	<b>4.89</b>	19.38
FocalNet	2.05	2.07	4.28	4.40	2.06	4.40	19.26
Flux Not COT (Split)	0.84	0.83	<b>4.81</b>	4.83	0.84	4.83	16.98

Table 2. Comparison of qualitative metrics across methods.



Figure 2. Comparison of defogging results on a real foggy image. The model trained on synthetic fog (DehazeFormer) shows color distortion and overcorrection, while the Flux CoT model better restores object visibility and preserves natural appearance, highlighting the domain gap between synthetic and real fog.

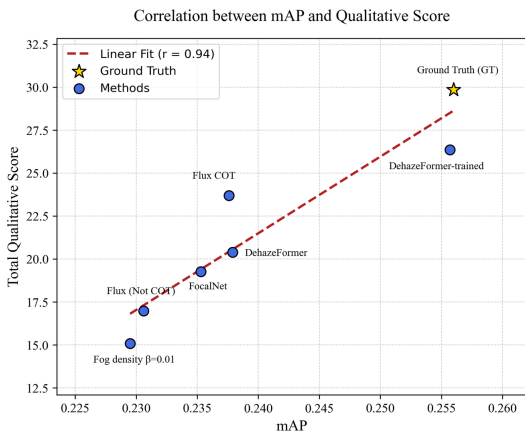


Figure 3. Correlation of mAP and qualitative scores across models. Ground truth provides the upper bound for both metrics. The two measures are strongly correlated ( $r = 0.94$ ), indicating that qualitative evaluation aligns closely with quantitative detection performance.

t/relation consistency are weaker. This supports our CoT design that emphasizes boundary sharpness and local contrast.

**Real vs. synthetic fog.** As shown in Table 1, training defogging models on synthetic fog datasets can yield strong performance. For example, the model trained on Cityscapes synthetic fog achieves substantial improvements over the foggy baseline in downstream detection and segmentation metrics. However, qualitative inspection of real-world hazy or foggy images (see Figure 2) reveals a lack of generalization: real fog images processed by the Cityscapes-trained model exhibit noticeable color shifts, artifacts, and overcorrection. Thus, while synthetic training delivers high quantitative performance, it often fails to produce usable models for deployment in real-world scenarios. This behavior suggests that learning to invert the specific fog-generation functions employed in synthetic datasets does not ensure that the network captures the broader statistical or physical properties of real fog. In practice, synthetic fog datasets typically generate fog using pseudo-random functions with additive noise overlays. Although such methods produce visually similar images, they fall short of accurately modeling the physical characteristics of real fog. As a result, models trained on synthetic data may learn to invert these artificial processes effectively, but their learned mappings break down when confronted with fog that does not follow the same generative assumptions.

## 7. Conclusion

In this work, we presented a comprehensive empirical study of defogging pipelines for autonomous driving perception. By benchmarking classical filters, modern learning-based restoration models, chained variants, and prompt-driven VLM editors, we systematically analyzed their impact on both image quality and downstream detection and segmentation tasks. Our results demonstrate that while synthetic training can deliver high quantitative gains, these improvements often fail to generalize to real-world fog, underscoring the limitations of current synthetic datasets. We further showed that chaining filters with models can yield either complementary benefits or compounding artifacts, depending on the order of operations, and that VLM-based editors provide a flexible alternative but remain inconsistent in downstream performance. Finally, our use of rubric-based VLM judgments highlights a promising path for aligning qualitative human-like assessments with quantitative task metrics. Together, these findings establish a transparent benchmark for evaluating defogging methods and emphasize the need for approaches that bridge the gap between synthetic training and robust real-world deployment.

## References

- [1] Armin Abdollahi, Negin Ashrafi, Xinghong Ma, Jiahao Zhang, Daijia Wu, Tongshou Wu, Zizheng Ye, and Maryam Pishgar. Advanced predictive modeling for enhanced mortality prediction in icu stroke patients using clinical data. *PLoS One*, 20(5):e0323441, 2025. 3
- [2] Negin Ashrafi, Armin Abdollahi, Jiahong Zhang, and Maryam Pishgar. Optimizing mortality prediction for icu heart failure patients: Leveraging xgboost and advanced machine learning with the mimic-iii database. *arXiv preprint arXiv:2409.01685*, 2024. 3
- [3] Stephen Batifol, Andreas Blattmann, Frederic Boesel, Saksham Consul, Cyril Diagne, Tim Dockhorn, Jack English, Zion English, Patrick Esser, Sumith Kulal, et al. Flux. 1 kontext: Flow matching for in-context image generation and editing in latent space. *arXiv e-prints*, pages arXiv–2506, 2025. 3
- [4] Mario Bijelic, Tobias Gruber, Faisal Mannan, Florian Kraus, Werner Ritter, Klaus Dietmayer, and Felix Heide. Seeing through fog without seeing fog: Deep multimodal sensor fusion in unseen adverse weather. In *Proceedings of the IEEE Conference on Computer Vision and Pattern Recognition (CVPR)*, pages 11682–11692, 2020. 1, 2
- [5] Bolun Cai, Xiangmin Xu, Kui Jia, Chunmei Qing, and Dacheng Tao. Dehazenet: An end-to-end system for single image haze removal. *IEEE Transactions on Image Processing*, 25(11):5187–5198, 2016. 1, 2
- [6] Bowen Cheng, Alexander G. Schwing, and Alexander Kirillov. Masked-attention mask transformer for universal image segmentation. In *Proceedings of the IEEE/CVF Conference on Computer Vision and Pattern Recognition (CVPR)*, pages 1290–1299, 2022. 1, 6
- [7] Marius Cordts, Mohamed Omran, Sebastian Ramos, Timo Rehfeld, Markus Enzweiler, Rodrigo Benenson, Uwe Franke, Stefan Roth, and Bernt Schiele. The cityscapes dataset for semantic urban scene understanding. In *Proceedings of the IEEE Conference on Computer Vision and Pattern Recognition (CVPR)*, pages 3213–3223, 2016. 6
- [8] Hugging Face. Diffusers: Controlnet training pipeline examples. <https://github.com/huggingface/diffusers/tree/main/examples/controlnet>, 2023. Commit <commit-hash> accessed on September 19, 2025. 1, 5
- [9] Yifan Fan, Yuxin Wang, Ming Wei, Feilong Lin Wang, and Hui Xie. Friendnet: Detection-friendly dehazing network. *arXiv preprint arXiv:2403.04443*, 2024. 2
- [10] Arya Fayyazi, Mehdi Kamal, and Massoud Pedram. Fair-sight: Fairness assurance in image recognition via simultaneous conformal thresholding and dynamic output repair. *arXiv preprint arXiv:2504.07395*, 2025. 3
- [11] Alireza Golkarieh, Parsa Razmara, Ahmadreza Lagzian, Amirhosein Dolatabadi, and Seyed Jalaleddin Mousavirad. Semi-supervised gan with hybrid regularization and evolutionary hyperparameter tuning for accurate melanoma detection. *Scientific Reports*, 15(1):31977, 2025. 3
- [12] Song Han, Huizi Mao, and William J. Dally. Deep compression: Compressing deep neural networks with pruning, trained quantization and huffman coding. In *International Conference on Learning Representations (ICLR)*, 2016. 3
- [13] Kaiming He, Jian Sun, and Xiaoou Tang. Single image haze removal using dark channel prior. *IEEE Transactions on Pattern Analysis and Machine Intelligence*, 33(12):2341–2353, 2011. 1, 2
- [14] Kaiming He, Georgia Gkioxari, Piotr Dollár, and Ross Girshick. Mask r-cnn. In *Proceedings of the IEEE International Conference on Computer Vision (ICCV)*, pages 2961–2969, 2017. 4
- [15] Ari Holtzman, Jan Buys, Li Du, Maxwell Forbes, and Yejin Choi. The curious case of neural text degeneration. In *International Conference on Learning Representations*, 2020. 3
- [16] Po-Wei Hsieh, Yu-Chiang Frank Wang, and Yung-Yu Chuang. Variational contrast–saturation enhancement

- model for visibility restoration. *Signal Processing*, 194:108404, 2022. 2
- [17] Liwei Huang, Bitao Jiang, Shouye Lv, Yanbo Liu, and Ying Fu. Deep-learning-based semantic segmentation of remote sensing images: A survey. *IEEE Journal of Selected Topics in Applied Earth Observations and Remote Sensing*, 17:8370–8396, 2023. 4
- [18] Junaid Iqbal, Rizwan Hafiz, and Mubarak Ali. Fogadapt: Self-supervised domain adaptation for semantic segmentation of foggy images. *arXiv preprint arXiv:2201.02588*, 2022. 2
- [19] Tina Khezresmaeilzadeh, Parsa Razmara, Seyedarmin Azizi, Mohammad Erfan Sadeghi, and Erfan Baghaei Potraghloo. Vista: Vision-language inference for training-free stock time-series analysis. *arXiv preprint arXiv:2505.18570*, 2025. 3
- [20] Thomas N. Kipf and Max Welling. Semi-supervised classification with graph convolutional networks. In *International Conference on Learning Representations (ICLR)*, 2017. 3
- [21] Alexander Kirillov, Kaiming He, Ross Girshick, Carsten Rother, and Piotr Dollár. Panoptic segmentation. In *Proceedings of the IEEE/CVF Conference on Computer Vision and Pattern Recognition (CVPR)*, pages 9404–9413, 2019. 1, 4
- [22] Alexander Kirillov, Tsung-Yi Lin, Piotr Dollár, Ross Girshick, Kaiming He, and the COCO Consortium. Coco panoptic segmentation api (panopticapi). <https://github.com/cocodataset/panopticapi>, 2019. Accessed: 2025-09-18. 6
- [23] Hae Beom Lee, Seung Hwan Han, Jong-Hwan Oh, Se-Young Oh, Jinkyu Kim, and Minyoung Kim. Prometheus-vision: Vision-language model as a judge for fine-grained evaluation. *arXiv preprint arXiv:2401.06591*, 2024. 4
- [24] Quentin Lhoest, Clément Delangue, Patrick von Platen, Thomas Wolf, et al. The hugging face hub: An open platform for sharing machine learning models, datasets, and metrics. *Journal of Machine Learning Research*, 23(1):1–7, 2022. 1, 6
- [25] Boyi Li, Xiulian Peng, Zhangyang Wang, Jinhui Xu, and Dan Feng. Aod-net: All-in-one dehazing network. In *Proceedings of the IEEE International Conference on Computer Vision (ICCV)*, pages 4770–4778, 2017. 1, 2
- [26] Boyi Li, Wenqi Ren, Jianqiang Zhang, Dongwei Yu, Xiaojie Cao, and Dacheng Tao. End-to-end united video dehazing and detection. In *Proceedings of the AAAI Conference on Artificial Intelligence (AAAI)*, 2018. 2
- [27] Boyi Li, Wenqi Ren, Dengpan Fu, Dacheng Tao, Dan Feng, Wenqi Wang, Wei Zeng, and Zhangyang Wang. Benchmarking single-image dehazing: Toward real-world deployment. *IEEE Transactions on Image Processing*, 28(1):492–505, 2019. 1, 2
- [28] Xiaohong Liu, Yongrui Ma, Zhihao Shi, and Jun Chen. Griddehazenet: Attention-based multi-scale network for image dehazing. In *Proceedings of the IEEE International Conference on Computer Vision (ICCV)*, pages 7314–7323, 2019. 2
- [29] Jonathan Long, Evan Shelhamer, and Trevor Darrell. Fully convolutional networks for semantic segmentation. In *CVPR*, 2015. 4
- [30] Xiaofeng Ma, Yanchao Zhang, Dongdong Sun, Zhizhong Zhang, Haibo Huang, Yajing Li, and Xiaofei Li. Both style and fog matter: Cumulative domain adaptation for semantic foggy scene understanding. In *Proceedings of the IEEE Conference on Computer Vision and Pattern Recognition (CVPR)*, pages 18954–18963, 2022. 2
- [31] Ninareh Mehrabi, Fred Morstatter, Nripsuta Saxena, Kristina Lerman, and Aram Galstyan. A survey on bias and fairness in machine learning. *ACM Computing Surveys*, 54(6):115:1–115:35, 2021. 3
- [32] Mahtab Movahhedrad, Zijing Chen, and C-C Jay Kuo. A green learning approach to efficient image demosaicking. In *2024 IEEE International Conference on Big Data (BigData)*, pages 1067–1074. IEEE, 2024. 3
- [33] Duc Ngo, Sungdae Yang, Hyunsung Kim, and Deokwoo Park. Visibility restoration: A systematic review and meta-analysis. *Sensors*, 21(8):2625, 2021. 2
- [34] Erfan Baghaei Potraghloo, Seyedarmin Azizi, Souvik Kundu, and Massoud Pedram. Top-h decoding: Adapting the creativity and coherence with bounded entropy in text generation. *arXiv preprint arXiv:2509.02510*, 2025. 3
- [35] Xin Qin, Zhilin Wang, Yu Bai, Xiaodong Xie, and Huizhu Jia. Ffa-net: Feature fusion attention network for single image dehazing. In *Proceedings of the AAAI Conference on Artificial Intelligence (AAAI)*, pages 11908–11915, 2020. 1, 2
- [36] Zia-ur Rahman, Daniel J Jobson, and Glenn A Woodell. Multi-scale retinex for color image enhancement. In *Proceedings of IEEE International Conference on Image Processing (ICIP)*, 1996. 1, 2
- [37] Zia-ur Rahman, Daniel J Jobson, and Glenn A Woodell. Resiliency of the multiscale retinex image enhancement algorithm. Technical report, NASA, 1998. 2
- [38] Parsa Razmara, Tina Khezresmaeilzadeh, and B Keith Jenkins. Fever detection with infrared thermography: Enhancing accuracy through machine learning techniques. In *2024 IEEE EMBS International Conference on Biomedical and Health Informatics (BHI)*, pages 1–8. IEEE, 2024. 3

- [39] Samuel Rey, Hamed Ajorlou, and Gonzalo Mateos. Convolutional learning on directed acyclic graphs. In *2024 58th Asilomar Conference on Signals, Systems, and Computers*, pages 423–427. IEEE, 2024. 3
- [40] Christos Sakaridis, Dengxin Dai, and Luc Van Gool. Semantic foggy scene understanding with synthetic data. *International Journal of Computer Vision*, 126(9):973–992, 2018. 1, 2
- [41] Christos Sakaridis, Hao Wang, Ke Li, and Luc Van Gool. Acdc: The adverse conditions dataset with correspondences for robust semantic driving scene perception. In *Proceedings of the IEEE International Conference on Computer Vision (ICCV)*, pages 10765–10775, 2021. 1, 2
- [42] Yulun Song, Li He, Qingnan Chen, and Chunjing Ma. Vision transformers for single image dehazing (dehazeformer). *arXiv preprint arXiv:2204.03883*, 2022. 2
- [43] Google AI Studio. Google AI Studio, 2025. 3
- [44] Voxel51. Fiftyone: A tool for building high-quality datasets and visual ai projects. <https://github.com/voxel51/fiftyone>, 2025. Accessed: 2025-09-19. 6
- [45] Thomas Wolf, Lysandre Debut, Victor Sanh, Julien Chaumond, Clement Delangue, Anthony Moi, Pierric Cistac, Tim Rault, Rémi Louf, Morgan Funtowicz, Joe Davison, Sam Shleifer, Patrick von Platen, Clara Ma, Yacine Jernite, Julien Plu, Canwen Xu, Teven Le Scao, Sylvain Gugger, Mariama Drame, Quentin Lhoest, and Alexander M. Rush. Transformers: State-of-the-art natural language processing. In *Proceedings of the 2020 Conference on Empirical Methods in Natural Language Processing: System Demonstrations*, pages 38–45, 2020. 1, 6
- [46] Dilek M Yalcinkaya, Arian M Sohi, Khalid Youssef, Luis F Zamudio, Michael Elliott, Venkateshwar Pol sani, Rohan Dharmakumar, Robert Judd, Matthew S Tong, Dipan J Shah, et al. Physics-informed deep learning model selection for robust segmentation of multi-center stress perfusion datasets: results from the scmr registry. *Journal of Cardiovascular Magnetic Resonance*, 27, 2025. 4
- [47] Yuxin Zhang, Chao Xu, Wenbo Zhu, et al. Frequency-oriented transformer for remote sensing image dehazing. *Remote Sensing*, 16(3):454, 2024. 2
- [48] Chuan Zheng, Xiaohong Xu, Xiangyu He, Fuming Yang, Wei Chen, and Liang Lin. Ultra-high-definition image dehazing via multi-guided bilateral learning. In *Proceedings of the IEEE Conference on Computer Vision and Pattern Recognition (CVPR)*, pages 16182–16191, 2021. 2
- [49] Karel Zuiderveld. Contrast limited adaptive histogram equalization. In *Graphics gems IV*, pages 474–485. Academic Press, 1994. 2